Estimation of rock mass strength using the synthetic rock mass (SRM) approach and particle flow modelling

A. Huaman and E. Hormazabal
SRK Consulting Chile

Significant developments in numerical modelling have been achieved during the last decade, but validation of these techniques is required to build up confidence. As these developments represent a significative advance for mining geomechanics, this paper focuses on the application of the relatively recent 3D particle flow code (PFC3D) using the synthetic rock mass (SRM) approach to simulate the mechanical behaviour of not only intact rock, but also rock masses. In this approach, rock mass samples are generated and tested by using these techniques; the obtained rock mass strength assessment is then cross-checked and compared to results obtained from applying empirical and worldwide-accepted rock mass strength criteria such as Hoek-Brown. The main rock properties of the samples to be analysed include the mechanical response under triaxial stress conditions, anisotropy, modulus, damage threshold, and peak strength. Finally, it is worth mentioning that when using the Hoek-Brown strength criterion, the strength envelope curve for each rock mass sample is generated based on input parameters *m* and *a* that are measured from triaxial testing of the intact rock.

Introduction

New techniques to estimate the strength of rock have arisen during the last decade. This paper is intended to improve confidence in the methodology known as the synthetic rock mass (SRM) approach and the particle flow code (PFC3D) (Mas Ivars *et al*., 2007, 2011; Itasca, 2008). Such techniques use the bonded particle model (BPM) (Potyondy and Cundall, 2004) to represent the intact rock behaviour as well as the smooth-joint contact model (SJM) (Mas Ivars *et al*., 2008a) for the representation of the discontinuities within the rock mass. In this sense, this work also intends to make a contribution towards the improvement of the efficiency, robustness, and usability of the abovementioned methods.

Moreover, nowadays the rock mass strength and the associated rock deformation and anisotropy is typically assessed based on empirical criteria. For instance, rock mass strength and deformation are usually computed utilizing the Hoek-Brown (H-B) strength criterion (Hoek *et al*., 2002), which is based not only on the intact rock properties, but also on the selection of a geological strength index (GSI) (Hoek, 1994). In addition, it is important to stress that it is not common to test rock mass samples in the laboratory, as it is an expensive and time-consuming activity.

The influence of rock compositional variability, and size and shape of rock blocks on techniques consisting of micro-modelling (PFC and SRM) needs to be further investigated as these factors are considered to govern the rock mass strength (Hoek, 2013; Read and Stacey, 2009). Cross-checking the results from such numerical techniques against widely accepted empirical approaches such as the Hoek-Brown strength criterion is then required for validation. In this sense, the scope of this article is mainly oriented towards the development of activities intended to supplement the cross-checking activities. It is worth mentioning that when using the Hoek-Brown strength criterion, the strength envelope curve for each rock mass sample is generated based on input parameters *m* and *a* that are measured from triaxial testing of the intact rock according to recommendations made by Mostyn and Douglas (2000). These authors demonstrated that the value for the a_i parameter in the intact rock is not always 0.5, and m_i is not a function of rock type; their work also proposed equations to estimate H-B input parameters from results of triaxial testing on intact rock.

Even though the scale effect on rock mass strength should also be investigated, as stressed by Mas Ivars (2010), this topic will not be studied in detail. The reader should note that the intact rock model development and calibration to resemble the actual mechanical behaviour observed in the laboratory is outside the scope of this work, and therefore it will only be considered as an input. Planes of weakness such as joints and minor faults are taken from a previously developed discrete fracture network (DFN) model; these structures are then introduced into the intact rock model to obtain representative rock mass samples of the real field-observed rock masses. Samples are tested considering a standard laboratory stress path in PFC3D to obtain the strength, σ_1, under three different confining stresses, σ_3, 0.2, 0.5,

and 1.0 MPa. Finally, the strength anisotropy for samples with one single joint is also modelled and compared to the theoretical approach proposed by Jaeger and Cook (1979). Owing to project confidentiality issues, the geological features and geotechnical descriptions of the rock samples are not further discussed.

Background

Triaxial test

Virtual tests were undertaken according to the specifications outlined by the International Society for Rock Mechanics (ISRM). Some features to be taken into account:

- A three-dimensional stress state exists, defined by three principal stresses, σ_1, σ_2, and σ_3 such that $\sigma_1 \neq \sigma_2 = \sigma_3$
- Failure occurs as the major principal stress is increased while the intermediate and minor principal stresses are kept constant.

Note that it is assumed that the intermediate stress has little effect on the sample behaviour under triaxial test conditions. Even though authors such Brady and Brown (2004) recommend polyaxial testing to overcome this pitfall and cite studies in which this assumption has proven not to be always correct; they also agree that triaxial test equipment is not required to be too specialized as this test might produce very similar results to those obtained under polyaxial conditions if it is properly carried out.

Strength anisotropy under triaxial compression

The anisotropic strength and deformational behaviour of rock have been extensively discussed in the literature. Studies carried out by Mas Ivars (2010), Donath (1972), and McLmore and Gray (1967) have even included laboratory triaxial testing of intact specimens. These approaches are illustrated by Brady and Brown (2004) and are presented in Figures 1 and 2. Note that the strength varies continuously with the angle of weakness plane with respect to direction of loading (β), as proven by different studies such as Brown et al. (1977) and Salcedo (1983).

Typically, for rock mass strength, two approaches are considered: parallel through-going discontinuities and the Hoek-Brown empirical failure criterion. The former approach is based on the work of Jaeger and Cook (1979), who introduced an analysis of rock masses with a single discontinuity inclined with respect to the principal stresses as shown in Figure 1a. The criteria for this approach are shown in Equations [1] and [2]; note that the Mohr-Coulomb (M-C) relationship (cohesion, c_w, and friction, φ_w) were considered. The main outcome is the theoretical strength anisotropy curve as presented in Figure 1b.

Equation [1] Derived equation in this approach:

$$(\sigma_1 - \sigma_3) = \frac{2(c_w + \sigma_3 \tan\phi_w)}{(1 - \tan\phi_w \cot\beta)\sin 2\beta}$$

Equation [2] β angle at which the minimum strength occurs:

$$\tan 2\beta = -\cot\phi_w \quad \text{or} \quad \beta = \frac{\pi}{4} + \frac{\phi_w}{2}$$

Slip will not occur as:

$\beta \rightarrow 90°$ and $\beta \leq \phi$

where:

σ_1: Major principal stress
σ_3: Minor principal stress
β: Joint inclination (refer to Figure 1a)
φ: Friction angle.

It is worth mentioning that several authors (Sainsbury and Sainsbury, 2013; Douglas, 2002) stress that this approach does not resemble the real behaviour when considering a set of discontinuities rather than a single discontinuity. In fact, for a single discontinuity, a U-shape with two shoulders is obtained, whereas for a set of discontinuities a U-type anisotropy curve is generated with no shoulders (Figure 1).

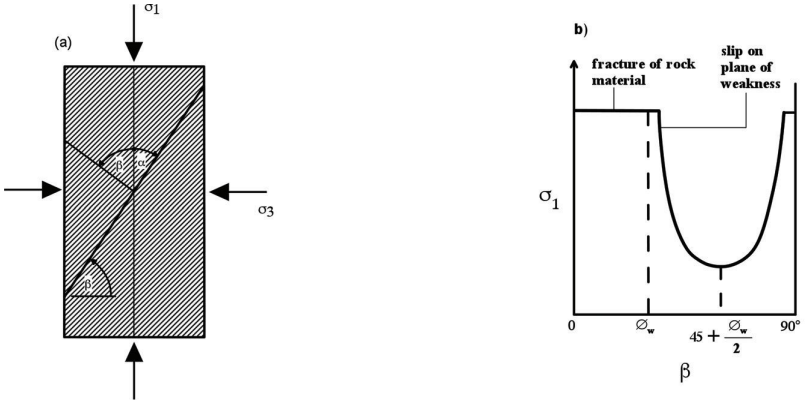

Figure 1 – Typical strength anisotropy curve for samples with a single discontinuity under triaxial conditions. (Brady and Brown, 2004)

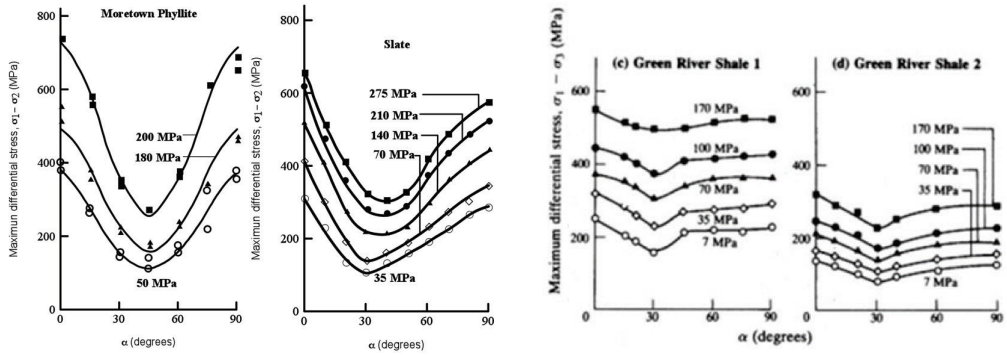

Figure 2 – Laboratory testing conducted on anisotropic intact laboratory samples: (a) phyllite, (b-d) slate and two shales, (McLamore and Gray, 1967; in Brady and Brown, 2004)

Hoek-Brown strength criterion

The Hoek-Brown approach is an empirical-based failure criterion to assess the strength of rock masses (*i.e*. rock masses that are not structurally controlled) (Hoek and Brown, 1980). A curved envelope is used to represent such strength and it is usually presented in terms of the major and minor principal stresses (Equation [3]). Although the Hoek-Brown criterion was initially developed for underground excavations in hard rock, it has been revised in order to evaluate weaker rock masses (Hoek and Marinos, 2007). The development accounts for not only the intact rock properties (degree of fracturing), but also the joint conditions within the rock mass, which are factors that govern the strength behaviour. This criterion utilizes the geological strength index (GSI) to better relate the failure criterion with geological observations and to consider the scale effect on the rock mass. According to Hoek (2007), 'the strength of a jointed mass depends on the properties of the intact rock pieces, as well as the freedom of the rock pieces to slide and rotate under different stress conditions'. The input parameters in this criterion are shown in Table I.

$$\sigma_1' = \sigma_3' + \sigma_{ci}\left(m_b\frac{\sigma_3'}{\sigma_{ci}'} + s\right)^a$$

Equation [3] Hoek-Brown criterion

$$\sigma_t = -\frac{s\sigma_{ci}}{m_b}$$

Equation [4] Tensile strength

Table I. Input parameters for the Hoek-Brown Strength criterion

Parameter	Description	For intact rock		For rock mass (Hoek *et al.*, 2002)	
m^*	Material parameter, related to the steepness of the τ – σ curve, similar to ø.	m_i	Values are recommended to be taken from testing rather than empirical tables.	m_b	$\frac{m_b}{m_i} = \exp\left(\frac{GSI-100}{28-14D^{**}}\right)$
a	Factor related to the curvature of the σ_1 and $\sigma_3$relationship.	a_i	0.5 for intact rock. According to Hoek, it varies from 0.5 to 0.65	a_b	$a = \frac{1}{2} + \frac{1}{6}\left(e^{-GSI/15} - e^{-20/3}\right)$
s	Material parameter very roughly related to the cohesion (c) represented by the tensile strength.	s_i	$s = \exp\left(\frac{GSI-100}{9-3D}\right)$	s_b	$s = \exp\left(\frac{GSI-100}{9-3D}\right)$
σ_c	Uniaxial compressive strength	σ_{ci}	-	σ_c	$\sigma_c = \sigma_{ci} \cdot s^a$

* *m* and *a* are assumed to be independent according to this criterion.
** *D* is a factor that depends upon the degree of disturbance to which the rock has been subjected.

It is worth mentioning that initially the scale effect on intact rock was believed to be related to factors such as sample preparation or due to the presence of microfractures. However, studies considering PFC3D modelling (Tagliabue, 2012) show that such effect might be a product of the interaction of the grains and the effect of cracks on the rock sample. Finally, the reader should note that different authors such as Brady and Brown (2004), Wyllie and Mah (2004) have agreed that the Hoek-Brown scale effect equation may not properly estimate the strength of rock.

Numerical modelling

Particle flow modelling - Itasca PFC3D

PFC3D is a discontinuum code developed by Itasca Consulting (2008) that models interaction of discrete objects, as it is able to simulate complicated problems in solid mechanics and granular flow. By default, spherical particles are assembled to create models. Not only objects that present brittle behaviour, but also those that exhibit large-strain and/or fracturing are suitable to be modelled by this code. PFC3D can also be used to analyse the dynamic behaviour of a particulate system.

Even though this technique has proven to provide realistic results when simulating laboratory tests on intact rock as well as on rock masses, only tests on rock mass samples will be presented and analysed in this work. The authors have also run tests on intact rock samples to investigate the scale effect, and main findings so far will be presented, but results and discussion on this topic are outside the scope of this work.

Potyondy and Cundall (2004) initially proposed a methodology to generate intact rock models in PFC3D in which the rock is represented by a cemented granular material or irregularly shaped materials that may break when its strength is reached. The procedure consists of the following steps: Particle Assembly, Install Isotropic Stresses, Floater Elimination, Install Parallel Bond, and Clustering (Figure 3). In the rocks studied in this investigation, the cementation between particles in PFC3D is represented by parallel bonds (Figure 4), which can resist normal forces as well as moments about the particle's axis.

The main advantages of PFC3D over other codes include the potential to be more efficient, as contact detection between circular objects is much simpler than contact detection between angular objects. Secondly, there is no limit to the magnitude of displacement; finally, bonded blocks might break. The use of the smooth-joint contact model (SJM) (Mas Ivars *et al.*, 2008; Mas Ivars, 2010) in all the contacts between particles that lie upon opposite sides of the joints constitutes a practical solution to the fact that block boundaries are not planar in this code. This approach will be used to represent the discontinuities. Strain-softening models for discontinuities are common for modelling such structures and this incorporated into PFC3D (Itasca Consulting, 2008).

As mentioned before, a calibrated intact rock model is utilized as input in this paper; such a model has been developed to match the physical test results carried out on rock samples in uniaxial compression, indirect tension, and triaxial compression. The obtained micro-properties will only be partially presented (Table II) due to reasons of project confidentiality.

Table II. Main calibrated intact rock model micro-properties

Particle properties		
Property	Symbol	Values
Particle radius lower bound	rlo	1.5 mm
Particle radius upper bound	rhi	2.0 mm
Particle shear stiffness	ks	2.70E+07 Pa
Particle friction coeffient	fric	0.9

Bond properties		
Property	Symbol	Values
Parallel bond (PB) normal stiffness	Pb_kn	9.26E+11 Pa
PB shear stiffness	Pb_ks	4.63E+11 Pa
PB normal strength	Pb_nstren	8.00E+06 Pa
PB shear strength	Pb_sstren	4.80E+07 Pa

Finally, it is important to emphasize that by using the SJM, the role of block angularity and interlocking on rock mass strength and brittleness are better represented in numerical modelling as regarded by Mas Ivars (2010) and Itasca Consulting (2012). This statement reinforces the scope of this work regarding the comparison between PFC3D results and Hoek-Brown strength criterion since, as described by Hoek (2007), interlocking as well as surface conditions are considered the most influential factors within this empirical criterion.

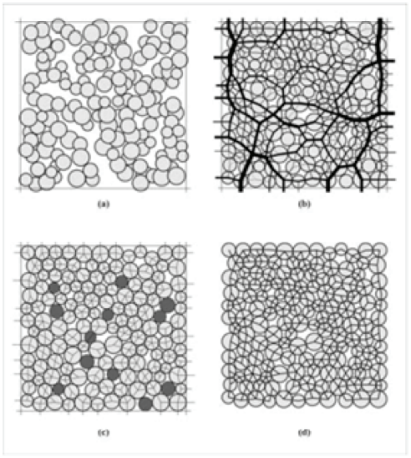

Figure 3 – According to Itasca consulting (2008) the material-genesis procedure includes: (a) particle assembly, (b) contact-force distribution, (c) floating particles, and (d) parallel-bond network

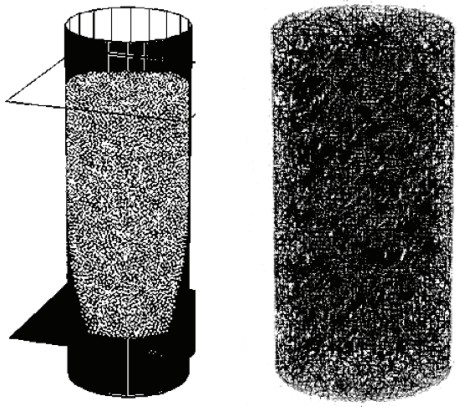

Figure 4 – Particle assemble step outcome and Installing isotropic stresses in the model

Nonlinear least-squares curve-fitting from laboratory data

Parameters for the Hoek-Brown strength will be calculated by utilizing the software RocData (Rocsience, 2014) to carry out nonlinear least-squares curve-fitting regression. Note that RocData provides the user with options for this regression; in this work, the Levenberg-Marquardt standard method will be utilized to perform such regression from test results of the intact rock model (GSI: 100).

As recommended by Mostyn and Douglas (2000), the parameters for intact rock (*mi* and *sigci*) should preferably be estimated from triaxial test on intact rock samples. Consequently, 21 test results (UCS and triaxial tests) were considered to obtain a value of 5.634 for *mi* and 14.291 MPa for *sigci*. Note that due to time constrains, UCS tests were simulated in PFC3D by simply running a triaxial test with a confining pressure equal to zero.

Joint model generation

Triaxial testing of samples containing discontinuities was carried out by assigning typical strength and stiffness macro-properties for discontinuities (c : 0 Pa and φ : 40°). Refer to Table II for more references on strength properties.

Rock mass sample generation

Based not only on the intact rock model, but also by using the smooth joint contact model, ten (10) synthetic rock mass samples were produced in PFC3D by explicitly including joints/shear orientations, properties, and other parameters according to a DFN model. Discontinuities were inserted considering not only a joint hierarchy and/or the cross-cutting relations between different joint sets, but also their relative age. In general, the joint interaction as well as the age determination was established as recommended by Harries (2001) and Mas Ivars (2010). Observed rock masses in the field are then resembled into synthetic models to be tested in PFC3D. Table III shows more information. Regarding the GSI selection, note that a range is selected for each sample and mean values are considered input parameters into further calculations throughout this work.

Table III . Simplified characterization of rock mass samples

ID	Joint sets	Faults/shears	Blockiness	Joint condition	Mean GSI
i	2	NA	Intact	Good	80
ii	3	NA	Blocky	Good	70
iii	3	NA	Blocky	Fair to good	65
iv	3	NA	Blocky to very blocky	Fair to good	60
v	4	NA	Blocky to very blocky	Fair to good	57
vi	4	Yes	Very blocky	Fair to poor	38
vii	4	NA	Very blocky	Fair to good	55
viii	4	Yes	Blocky/disturbed	Fair to poor	35
ix	7	NA	Very blocky to disturbed	Fair to good	50
x	7	Yes	Blocky/disturbed	Fair to poor	33

Material testing

The synthetic rock masses were tested by confining each cylindrical sample (comprised of a compacted particle assembly) and increasing the major principal stress until failure. The test will be developed as highlighted in the literature review. Note that the top and bottom walls simulate loading platens whereas the lateral cylinder wall simulates the confinement experienced by the sample; a numerical servomechanism maintains a constant confining stress within the sample. The load is applied in a strain-controlled fashion (Itasca, 2008); finally, the material response consisting of stresses, strains (including volumetric) and others is computed using the 'History' logic (inserting history points) in PFC3D and is monitored during each test.

Results and discussion

Intact rock strength

Table IV show results obtained from testing series not only of UCS tests on intact rock (100 mm diameter), but also triaxial tests of intact rock model (GSI:100 and 100 mm diameter). Results from 21 tests will be presented and analysed in this work.

Table IV . UCS and triaxial test results for intact rock model

	Sigma 3 (MPa)	Sigma 1 (MPa)	Mean Sigma1 (MPa)	Average crack initiation (MPa)	*E* (GPa)	Poisson's ratio
UCS	0	13.60	13.56	8.32	15.84	-
	0	13.59				
	0	13.48				
TRIAXIAL TEST	0.1	14.99	14.86	9.28	16.01	0.233
	0.1	15				
	0.1	14.58				
	0.2	15.59	15.42	9.46	15.98	0.225
	0.2	15.6				
	0.2	15.07				
	0.5	16.6	16.44	10.15	16.29	0.210
	0.5	16.61				
	0.5	16.1				
	1	18.14	17.98	11.11	16.53	0.19
	1	18.15				
	1	17.65				
	1.5	19.58	19.44	12.06	16.95	0.184
	1.5	19.59				
	1.5	19.16				
	2	21.07	20.97	12.99	17.14	0.177
	2	21.08				
	2	20.75				

The numerical modelling showed that peak strength increases as the confining pressure is increased. The mean compressive strength varies from 13.56 MPa up to 20.97 MPa under different confining stress varying from 0.1 MPa up to 2 MPa. Moreover, differences between results at the same confining stress are considered acceptable, therefore this data can be utilized to develop not only the Hoek-Brown criterion (regression curve fitting), but also to start carrying out triaxial tests on rock mass samples (note that only one DFN model was used). This difference might be assigned to the material generation procedure, which involves processes such as the particle assembly, size distribution, rearrangement of particles, as well as floater elimination, which are carried out by randomly selecting and/or creating particles with different radii; as a result, it may be posited that each model is slightly different. Finally, a quasi-brittle behaviour has been observed in each test, which is normally expected from intact rock models.

Intact rock strength anisotropy

Nine virtual tests were carried to investigate the transverse isotropic behaviour of samples with a single joint. Note that it is assumed that rock behaviour is structurally controlled by the single joint in these tests. The single joint strength and theoretical curve will be determined based on PFC3D modelling and the Jaeger and Cook (1979) approach respectively. Results are shown in Figure 5. It is worth noting that a value of 45° was considered for the friction angle of the joint regarding the theoretical approach as well as 1 MPa as the confining stress.

As shown in Figure 5, the rock behaviour observed in PFC3D is reasonably similar to that predicted by Jaeger and Cook (1979) in terms of the minimum and maximum compressive strength; however, the shape of the curve obtained is not the same. The theoretical curve slightly overestimates the compressive strength when the inclination angle of the single joint varies from 30 to 60 degrees. Moreover, according to the PFC3D results, there is no constant value for the strength at low and high values of (β) predicted by Jaeger and Cook (1979). This behaviour was also observed in the laboratory.

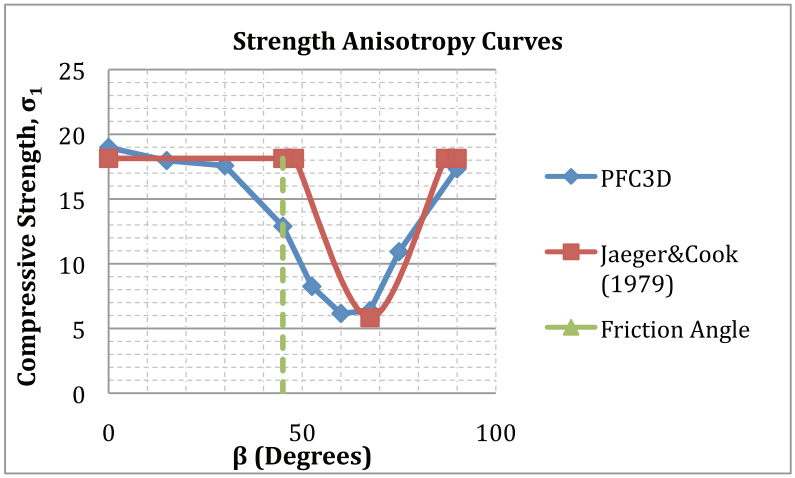

Figure 5 – Strength anisotropy curves obtained from (a) virtual testing in PFC3D, and (b) Jaeger and Cook (1979) approach

Using the angle (64 degrees) at which the minimum strength was calculated in PFC3, the internal friction angle may be estimated by using back-analysis through the equations posited by Jaeger and Cook (1979). As a result, a predicted internal friction angle of 38 degrees is estimated; note that this result validates the model as it is an acceptable value for joints in these types of rocks. PFC3D results also showed that failure through the discontinuity did not occur, not only when the angle of inclination was approaching 90 degrees, but also in the range of zero degrees to the friction value (45 degrees); in fact, shear failures through the grains were observed during the virtual test. In summary, it appears that the approach proposed by Jaeger and Cook (1979) does not reflect a proper estimation of strength variation at different inclination angles of the discontinuity; it generates an oversimplified anisotropic strength curve compared to PFC3D results.

Rock mass strength

Table V and Figure 6 summarize the results from using the H-B criterion on the rock mass samples, as well as results obtained from testing samples in PFC3D . Note that a value of zero for the *D* factor was considered.

Discussion

Figures 8 to 12 show graphs comparing computed PFC3D results to the envelope obtained from using the Hoek-Brown strength criterion. The observed post-failure behaviour for two samples is shown in Figure 13; these observations are compared to the suggested post-failure responses by Hoek (2007) for good- and poor-quality rock mass respectively.

Table V . Rock mass strength according to Hoek-Brown strength criterion

SAMPLE	Mean GSI	s_b	m_b	Sig_t (MPa)	a_b	UCS (MPa)	Sigma 1 (MPa)			
							Sigma3 0.2 MPa	Sigma3 0.5 MPa	Sigma3 1 MPa	Sigma3 2 MPa
Intact	100	1.000	5.634	2.537	0.500	14.291	15.044	16.136	17.874	21.112
1	80	0.108	2.758	0.562	0.501	4.698	9.058	10.266	12.115	15.412
2	70	0.036	1.930	0.264	0.501	2.687	4.583	5.893	7.749	10.860
3	65	0.020	1.614	0.181	0.502	2.029	3.765	5.077	6.890	9.889
4	60	0.012	1.350	0.124	0.503	1.529	3.497	4.805	6.597	9.547
5	57	0.008	1.213	0.099	0.504	1.289	2.677	3.943	5.628	8.373
6	37.5	0.001	0.605	0.023	0.513	0.404	2.025	3.194	4.723	7.212
7	55	0.007	1.129	0.085	0.504	1.150	2.448	3.689	5.329	7.996
8	35	0.001	0.553	0.019	0.516	0.344	1.879	3.013	4.494	6.909
9	50	0.004	0.945	0.058	0.506	0.861	2.078	3.258	4.803	7.317
10	32.5	0.001	0.506	0.016	0.519	0.292	1.748	2.846	4.279	6.622

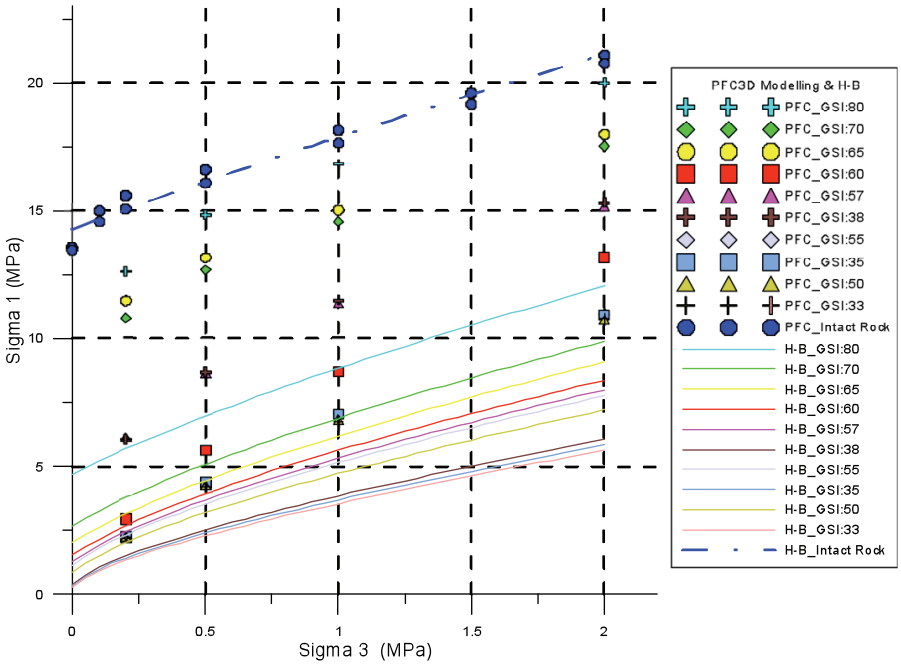

Figure 6 – Plot of results from numerical modelling in PFC3D and Hoek-Brown empirical criterion

Table VI. Rock mass strength results from virtual testing samples on PFC3D

ID	Mean GSI	Sigma 1 (MPa)			
		Sigma3 0.2 MPa	Sigma3 0.5 MPa	Sigma3 1 MPa	Sigma3 2 MPa
1	80	12.63	14.85	16.84	19.99
2	70	10.82	12.68	14.58	17.54
3	65	11.48	13.18	15.02	17.99
4	60	2.93	5.61	8.71	13.19
5	57	6.1	8.64	11.37	15.17
6	37.5	6.04	8.678	11.5	15.322
7	55	2.21	4.38	7.07	10.97
8	35	2.244	4.367	7.031	10.911
9	50	2.25	4.26	6.83	10.741
10	32.5	2.235	4.21	6.753	10.794

As initially expected, results from PFC3D on intact rock samples are lower than results from testing the intact rock model. The observed compressive strengths for the proposed rock mass samples in PFC3D were higher than those from the Hoek-Brown criterion. It also was noted that failure in the rock mass samples occurred through the rock mass rather than along any specific discontinuity, demonstrating that none of the sample failures were structurally controlled.

Conclusive results illustrate that for rock masses denoted as 'massive/intact' and 'blocky with good surface conditions', values from numerical modelling tend not to be located closely to the Hoek-Brown envelope curve; in fact, the Hoek-Brown strength results tend to be very conservative compared to the PFC3D results. On the other hand, for rock masses denoted as 'blocky to very blocky' or even for 'blocky and disturbed rock masses', results from the two different approaches tend to converge. The authors posit that the relatively considerable difference between H-B results criterion and PFC3D results are mainly due to the following:

1. Supporting data for such an empirical criterion is mainly from intact rock data, with little triaxial testing data of weak rock masses
2. The empirical Hoek-Brown criterion fails to consider the fracture persistence of joint fabric, as only interlocking and surface quality are taken into account to estimate the GSI value which governs all results. As mentioned in the literature review, particle flow modelling overcomes this pitfall, and therefore differences between results – PFC3D and H-B criterion – are obviously expected

3. The empirical H-B criterion assumes isotropic rock and rock mass behaviour. PFC3D results, on the other hand, have suggested that this assumption is not always correct
4. The GSI range exhibit a distribution about the mean. In the corresponding H-B curve, only mean values were taken into account
5. Uncertainty in specifying the *D* factor on the H-B strength criterion.

Moreover, as shown for poor-quality rock masses, under very low confining pressures (< 0.2 MPa), the Hoek-Brown strength criterion may slightly overestimate the real rock mass strength and may not be conservative enough for engineering purposes.

It is important to note that further work is required to assess the scale effect on rock mass samples considering different DFN models.

Analysis of the curvature (parameter a_b) of the σ_1 and σ_3 relationship

It can be observed from results that for good-quality rock masses, the parameter a_b from the H-B criterion seem to be too conservative as the resulting H-B curve is not close to results from PFC3D. In other words, the a_b parameter makes the compressive rock mass strength relatively conservative and therefore much lower values are obtained compared to results from PFC3D. On the other hand, for poor-quality rock masses, the curvature parameter a_b seems to yield a better fit with results from PFC3D. The authors recommend taking especial care in the GSI selection process as the a_b parameter is highly sensitive to GSI values.

Results also showed that H-B curves seem to produce similar results for very low confining pressures compared to those from PFC3D; in fact, as the confining stress tends to zero, the results from PFC3D are located either really close to or above the H-B curves. In summary, results have shown that even though there is still some validation of the PFC3D method to be carried out, PFC3D might be used with some degree of confidence to obtain the confining strength of rock masses when very low confining pressures are expected to be found *in situ*, or even to estimate the uniaxial compression strength.

Unfortunately, analysis of the influence of other parameters such as m_b or s_b on strength estimations considering the H-B criterion and its relation to PFC3D results could not be undertaken, as more laboratory results from PFC3D are required to generate a trend curve. If such test were performed, familiar shear-normal stress graphs ($\tau - \sigma$) would be obtained, and therefore a proper analysis of m_b and s_b could be carried out. A considerable improvement in computing power is expected in the forthcoming years, which will enable this analysis to be conducted.

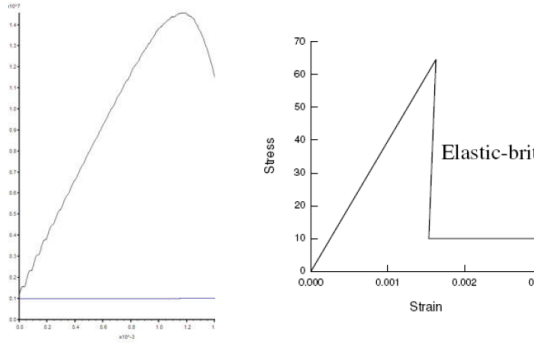

Figure 7 – Left: elastic quasi-brittle rock mass behaviour observed in good-quality rock masses (GSI>65); right: theoretical post-failure response of very good quality hard rock mass (Hoek, 2007)

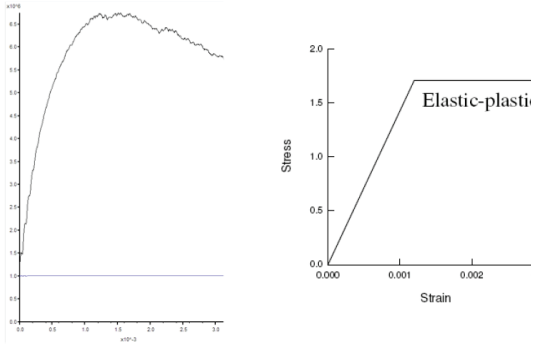

Figure 8 – Left: rock mass behaviour observed for poor-quality rock masses (GSI<50); right: theoretical post-failure response for very poor quality soft rock mass (Hoek, 2007)

Moreover, good-quality rock masses (GSI > 60) exhibit an elastic-quasi-brittle post-failure behaviour (Figure 7), whereas poor quality rock masses (GSI < 50) exhibit elastic-plastic post-failure behaviour (Figure 8). Note that these results are in good agreement with the suggested empirical post-failure characteristics for masses proposed by Hoek (2007). It was also noted that as the confining pressure was increased in each test, a transition from typically brittle behaviour (good-quality rock masses) to ductile behaviour (poor-quality masses) was generated. A possible explanation for this might be the introduction of geological structures with plastic mechanisms into rock mass samples and/or the grain-sliding effect. With respect to the rock mass behaviour, these factors are especially important when performing post- or progressive stress-strain behaviour analysis. Notwithstanding, validation for the PFC3D model has been obtained as good agreement has been shown between results from numerical analysis and the empirical criterion from

Hoek (2007). However, more triaxial data considering higher confining pressures is required to properly analyse the rock mass behaviour. More samples of differences sizes are also required to be tested to investigate any possible scale effect. Finally, it is important to point out that it is too soon to state that results from testing SRM samples should replace those from the H-B model. Further investigation is required with larger SRM samples, different DFN models, and lower joint friction angles.

Further work

The inherent limitation of the Hoek-Brown criterion, of not considering fracture persistence when characterizing the rock mass, should be further investigated in PFC3D. More studies are required to better validate the model when testing rock mass samples under more specific joint conditions (discontinuity, persistence (P21), infilling, *etc.*), especially considering geological structures such as bedding or cross-bedding. The associated joint hierarchy in the models should also be further investigated. Moreover, input parameters into the smooth joint contact model also need further validation, as well as the rock mass moduli. Further work is required to investigate the reasons why SRM estimation and H-B estimation do not coincide on occasions, as described in this article.

The possibility of using the presented methodology as a means of calibrating the Hoek-Brown strength envelope should also be investigated. As shown, the strength curve obtained by PFC3D can be used to derive the Hoek-Brown parameters.

The challenge for industry is to investigate the scale effect when virtual test results of relatively small rock mass samples are used to estimate the rock mass strength of larger regions. It is important to realize that increased computing power is required to explicitly analyse larger models such as mine-scale slopes in PFC3D.

Conclusions

Particle flow modelling, not only of intact rock strength but also of non-structurally controlled rock mass strength, was successfully carried out in order to resemble the mechanical behaviour of rock mass samples. The use of the smooth joint contact model to represent discontinuities in the rock mass has proven to be useful, as good agreement was found between data obtained from numerical modelling in PFC3D and results calculated from well-known strength approaches such as the empirical Hoek-Brown criterion and Jaeger and Cook (1979).

It has been proven that samples with a single joint are highly anisotropic. Results from PFC3D on samples of this type matched very well with the theoretical curve proposed by Jaeger and Cook (1979) in terms of minimum and maximum expected strength. However, this approach did not reflect a proper estimation of strength variation at different inclination angles of the discontinuity. It generates an oversimplified anisotropic strength curve compared to PFC3D results.

The Hoek-Brown criterion has been found to produce good results when dealing with good-quality rock masses; in fact, this work reinforces its validity and application when analysing these types of rock masses. Results were generally observed to be reasonably conservative compared to PFC3D results. However, for weak rock masses, results showed that the Hoek-Brown criterion may not be conservative enough to estimate the rock mass strength; in fact, it may be overestimating the real rock mass strength. Further validation of this statement is required. A postulated explanation for the observed difference includes factors such as the difference in supporting data for each approach, the ability to consider the fracture persistence of joint fabric on each approach, and the assumption of isotropic rock mass behaviour. In addition, the fact that the H-B strength results were obtained based on a GSI mean value rather than considering a range, as widely recommended, is considered to be influential in the presented comparison.

It is also worth mentioning that results from PFC3D agree with theory in that the observed rock mass strength decreases as joints are progressively inserted into the model. Moreover, post-failure behaviour observed in PFC3D showed a good agreement with the proposed post-failure mechanisms by Hoek (2007), not only for good-quality rock masses, but also for weak rock masses. A transition from typically brittle behaviour (good-quality rock masses) to ductile behaviour (poor-quality masses) was also recorded; however, more triaxial data considering higher confining pressures is required to properly analyse the rock mass behaviour. The results of this work have shown that even though there is still some validation of the PFC3D method to be carried out, PFC3D might be used with some degree of confidence to obtain the confining strength of rock masses when very low confining pressures are expected to be found *in-situ* or even to estimate the uniaxial compression strength.

Finally, it is important to point out that it is too soon to state that results from testing SRM samples should replace those from the H-B model. Further investigation is required with larger SRM samples, different DFN models, lower joint friction angles *etc*.

References

Bieniawski, Z.T. 1978. Determining rock mass deformability: experience from case histories. *International Journal of Rock Mechanics, Mining Sciences and Geomechanical Abstracts*, vol. 15. pp. 237-247.

Brady B.H.G. and Brown E.T. 2004, Rock Mechanics for Underground Mining. 3rd edn. Kluwer Academic Publishers, The Netherlands.

Brown, E.T., Richrads, L.R., and Barr, M.V. 1977 Shear strength characteristics of Delabole slates. *Proceedings of the Conference on Rock Engineering*, University of Newcastle-upon-Tyne, UK. Attewell, P.B. (ed.). pp. 33-51.

Cundall, P.A. and Strack, OD. 1979. A discrete numerical model for granular assemblies. *Geotechnique*, vol. 29, no. 1. pp. 47-65

Donath, F.A. 1972 Effects of cohesion and granularity on deformational models with physical observations -an approach to the estimation of rock mass behaviour. *Felsbau*, vol. 4, no. 4. pp. 197-202.

Douglas, K.J. 2002. Shear strength of rock masses, PhD thesis, School of Civil and Environmental Engineering, University of New South Wales, Australia.

Harries, N.J. 2001. Rock mass characterization for cave mine engineering. PhD thesis, University of Queensland, Australia.

Hoek, E. and Marinos, P. 2007. A brief history of the development of the Hoek-Brown failure criterion. *Soils and Rocks*, no. 2. November 2007. http://www.rocscience.com/education/hoeks_corner [Accessed September 2013].

Hoek, E. 1994. Strength of rock and rock masses. *ISRM News Journal,* vol. 2, no. 2. pp. 4-16.

Hoek E., Carranza-Torres, C.T., and Corkum B. 2002. Hoek-Brown failure criterion. *Proceedings of the North American Rock Mechanics Society (NARMS-TAC), Mining Innovation and Technology (Canada).* Bawden, H.R.W., Curran, J., and Telsenicki, M. (eds).

Hoek, E., Carter, T.G., and Diederichs, M.S.. 2013. Quantification of the Geological Strength Index Chart. *47th US Rock Mechanics / Geomechanics Symposium*. San Francisco, CA, USA.

Hoek, E. and Brown E.T. 1980 Empirical Strength criterion for rock masses, *Journal of the Geotechnical Engineering Division, ASCE*, vol. 106 (G79). pp. 1013-1035.

Hoek, E. 2007. Practical Rock Engineering, Chapter 12 Rock Mass Properties. www.rocscience.com

Hoek, E., Wood, D., and Shah, S. 1992. A modified Hoek-Brown failure criterion for jointed rock masses. *Proceedings of the ISRM Symposium on Rock Characterization: Eurock '92*, Chester, UK, 14-17 September 1992. Hudson, J.A. (ed.). Thomas Telford, London. pp. 209-213.

Itasca. 2008. PFC User's Manual. Itasca Consulting Group, Minneapolis.

Jaeger, J.C. and Cook, N.G.W. 1979. Fundamentals of rock mechanics. 3rd edn. Champman and Hall.

Mas Ivars, D. 2010 Bonded particle model for jointed rock mass. PhD thesis, Royal Institute of Technology (KTH), Stockholm, Sweden.

Mas Ivars, D., Deisman , N., Pierce, M., and Fairhurst, C. 2007. The synthetic rock mass approach—a step forward in the characterization of jointed rock masses. . *Proceedings of the 11th Congress of the International Society of Rock Mechanics*, vol. 1. Ribeiro e Sousa, L. and Grossmann, O. (eds). Taylor and Francis, London. pp. 485–490.

Mas Ivars D., Pierce M., DeGagne, D., and Darcel C. 2008a. Anisotropy and scale dependency in jointed rock-mass strength—A synthetic rock mass study. *Proceedings of the 1st International FLAC/DEM Symposium on Numerical Modeling*. Hart, R., Detournay, C., and Cundall, P. (eds). Paper 06-01.

Mas Ivars, D., Pierce, M.E., Darcel, C., Reyes-Montes, J., Potyondy, D.O., Young, R.P., and Cundall P.A. 2011. The synthetic rock mass approach for jointed rock mass modelling. *International Journal of Rock Mechanics and Mining Sciences*, vol. 48. pp. 219-244.

Mas Ivars, D., Potyondy, D.O., Pierce, M., and Cundall, P.A. 2008b. The smooth-joint contact model. *Proceedings of the 8th World Congress on Computational Mechanics and 5th European Congress on Computational Mechanics and Applied Science and Engineering*, Venice. Paper a2735.

McLamore, R. and Gray, K.E. 1967. The mechanical behaviour of anisotropic sedimentary rocks. *Journal of Energy for Industry, American Society of Mechanical Engineers*, Series B, vol.89. pp. 62-73.

Mostyn, G. and Douglas, K. 2000 Strength of intact rock and rock masses. *GeoEng2000, An International Conference on Geotechnical and Geological Engineering*, Melbourne, Australia, 19-24 November 2000. pp. 1389-1421.

Park, E-S, Martin, C.D., and Christiansson R. 2004. Simulation of the mechanical behaviour of discontinuous rock masses using a bonded-particle model. *Proceedings of the 6th North American Rock Mechanics Symposium*, Houston. Yale, D. *et al*. (eds). Paper ARMA 04-480.

Potyondy, D. O. and Cundall, P.A. 2004. A bonded-particle model for rock. *International Journal of Rock Mechanics and Mining Sciences*, vol. 41. pp. 1329-1364.

Read, J. and Stacey, P. 2009. Guidelines for open Pit Slope Design. 1st edn. CRC Press, Boca Raton, FL.

Sainsbury, D. and Sainsbury, B. 2013 Three-dimensional analysis of pit slope stability in anisotropic rock masses. *Slope Stability 2013*. Dight, P.M. (ed.). Australian Centre for Geomechanics, Perth.

Salcedo, D.A. 1983. Macizos Rocosos: Caraterizacion, Resitencia al Corte y Mecanimsmos de Rotura. *Proceedings, 25 Aniversario Conferencia Soc. Venezolana de Mecanica de Suelo e Ingenieria de Fundaciones*, Caracas. pp. 143-172.

Tagliabue, S. 2012. Investigation of intact rock scale effects using particle flow modelling. Honours thesis, School of Civil and Environmental Engineering, University of New South Wales.

Wyllie, D.C. and Mah, C.W. 2004. Rock Slope Engineering. 4th edn. Spon Press. New York, NY.

The Author

Andrés Huamán, *Geotechnical Engineer,* SRK Consulting (Chile)

Mr. Huamán is a Civil Engineer with a Master of Geotechnical Engineering and Engineering Geology. He has developed multidisciplinary projects acquiring practical knowledge in the fields of mining geotechnics and geology, rock and soil mechanics. He has experience in geotechnical site investigation, slope stability analysis, pit slope design, field inspections, excavations and drilling. He also has solid knowledge of different numerical methods and its application to geotechnical engineering. He recently has been involved on developing methodologies to evaluate bench berm designs through using site-collected data, stereographic analysis, Block theory and probabilistic methods for mine projects at different stages.